ELSEVIER

Polymer 43 (2002) 1343–1348

polymer

www.elsevier.com/locate/polymer

Dynamics of the leveling process of nanoindentation induced defects on thin polystyrene films

I. Karapanagiotis, D.F. Evans, W.W. Gerberich*

Department of Chemical Engineering and Materials Science, University of Minnesota, Minneapolis, MN 55455, USA

Received 24 April 2001; received in revised form 1 October 2001; accepted 3 October 2001

Abstract

Using Atomic Force Microscopy (AFM) we study the effect of nanoindentation induced defects on 50 and 120 nm thick unentangled polystyrene (PS) films, spin cast on silicon (Si) substrates. Indents with residual depths of penetration less than the film thickness level upon heating above the glass transition temperature (T_g) of bulk PS. The resulting leveling process is discussed in terms of a diffusion process driven by the curvature gradient. Calculated diffusivity values are close to the self-diffusivity of bulk PS.

Keywords: Polymer; Polymer physical chemistry; Polymer science

1. Introduction

Thin polymer films on hard or soft substrates have received significant attention due to their broad industrial utilization as protective coatings, lubricant layers and insulators in micro-circuits. Dewetting of the polymer is observed when the film is applied on a nonwetting surface and can result in failure of the device. Dewetting is initiated by indent-like surface fluctuations developed at the free surface of the polymer layer at temperatures higher than the glass transition (T_g) [1–14]. These spontaneous fluctuations are amplified with time resulting in the formation of small circular regions that expose substrate area to the air (dry patches). Pre-existing defects can play a role in determining the stability of polymer films, but this has received less systematic study. One source of such defects is airborne particles which have been identified as dewetting initiators [9]. Under the influence of gravitational forces or an attractive van der Waals interaction with the substrate, the particles sink through the film and upon reaching the substrate initiate dewetting. Defects induced by nanoindentation on the polymer film either initiate dewetting similarly to the spontaneous process or level resulting in a flat polymer surface.

In other studies we attempted to develop criteria that determine the indent evolution (dewetting or leveling) upon heating above T_g [15,16]. The dynamics of the indent amplification that results in dewetting has been studied earlier [9]. Here we focus on the dynamics of the (opposite) leveling process. The latter has been investigated mainly by numerical procedures [17,18]. Using Atomic Force Microscopy (AFM) the dynamics of the leveling process of unentangled polystyrene (PS) films spin cast on nonwettale silicon (Si) substrates is recorded on an experimental basis. In an earlier report, we investigated the leveling process of indents induced on different molecular weight PS films [19]. Here, we focus exclusively on unentangled PS films and we interpret the leveling process in terms of a diffusion process. We show that the calculated diffusivity values are comparable with the self-diffusivity of bulk PS.

2. Experimental section

Monodisperse PS (Polymer Labs, UK) with a molecular weight ($M_w = 10,900$ g/mol, $M_w/M_n = 1.02$, $T_g = 91$ °C) less than the critical entanglement molecular weight ($M_c = 38,000$ g/mol) was dissolved in spectroscopic grade toluene. Solutions were then filtered using 0.2 μm Teflon filters and spin cast onto 50 mm diameter silicon wafers (Virginia Semiconductor, Fredericksburg, VA). Solutions with concentrations of 2.5 and 5 wt% resulted in films with thicknesses, h, of 50 and 120 nm, respectively, measured by ellipsometry. The coatings were then annealed overnight in vacuum to remove residual solvent. The annealing temperatures were 60 °C for the thin ($h = 50$ nm) and 100 °C for the

* Corresponding author.
E-mail address: wgerb@umn.edu (W.W. Gerberich).

0032-3861/02/$ - see front matter
PII: S0032-3861(01)00688-7

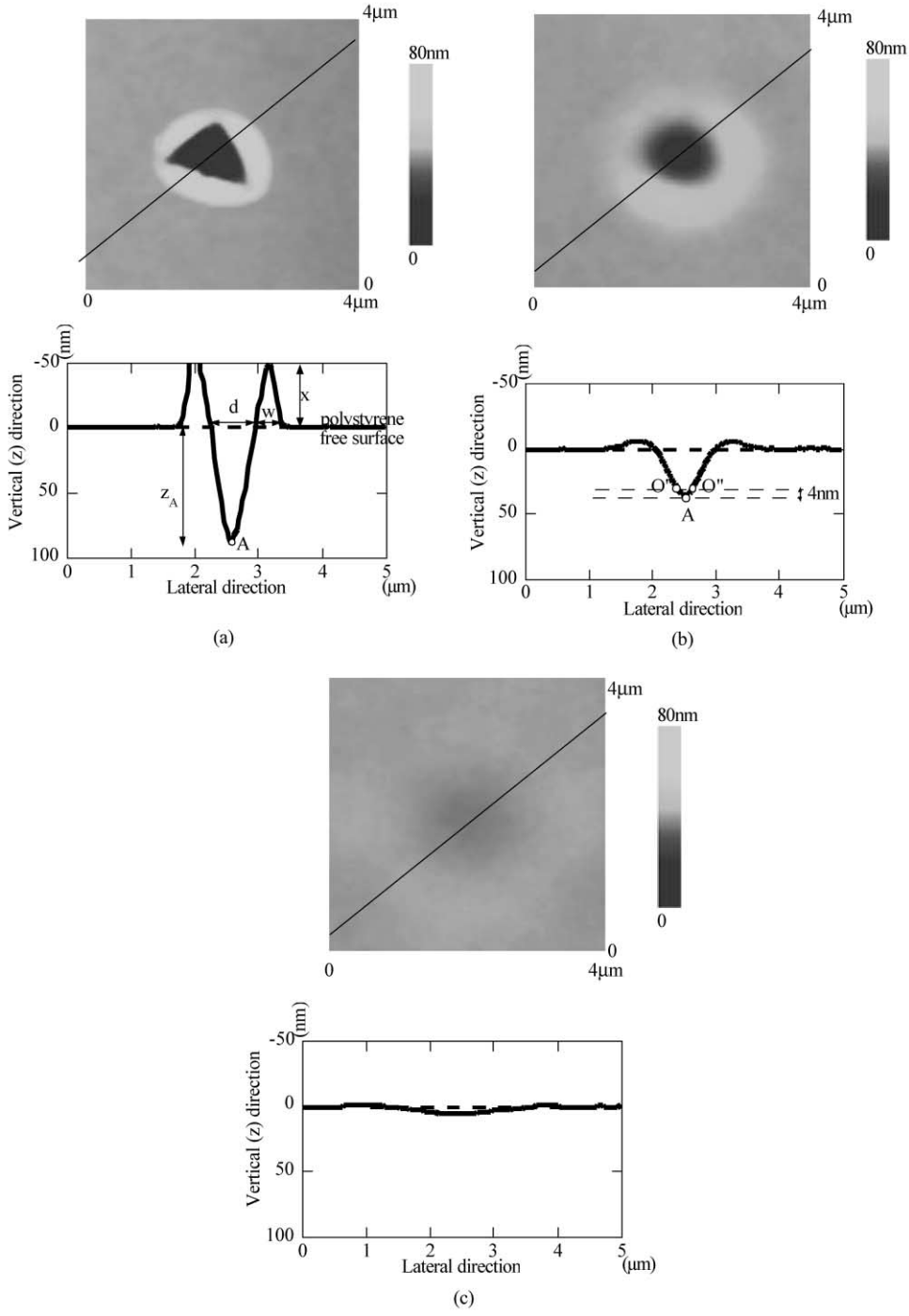

Fig. 1. AFM images and the corresponding cross-sections of a shallow indent (a) right after the indentation and before any thermal treatment above T_g ($t = 0$), (b) after heating at 100 °C for 42.5 min and (c) after heating at 100 °C for 175 min. The initial indent is triangular because a three-sided Berkovich pyramid tip was used during the nanoindentation. Upon heating, the shape changes to circular. The indent depth (z_A) and the rim height (x) decrease while the diameter (d) and the rim width (w) increase with time. The process tends to flatten the free polymer surface. The film thickness was 120 nm. Point A corresponds to the maximum indent depth.

thick ($h = 120$ nm) films. Upon heating above T_g, the thin films underwent spontaneous dewetting while the thick films were stable. The spin coating was performed in a clean room (class 10) to minimize particle contamination of the films. Si $<100>$ wafers were used as received. A native silicon oxide layer of 1.7 nm was detected by ellipsometry.

Triangular indents were imposed on the films using a nanoindentation Hysitron Triboscope (Hysitron Inc., Minneapolis, MN) apparatus mounted with a standard three sided pyramid (Berkovich) diamond tip with a 300 nm nominal radius of curvature. The nanoindentation device adapts to an AFM, which utilizes a Hysitron

microsensor system, instead of the standard AFM head component, for applying loads electrostatically. The Hysitron Triboscope is a load controlled instrument and the loads required to induce shallow indents with depths of penetration lower than the film thicknesses, were obtained by AFM imaging of a series of indentations. After the indentation, the defects were imaged at room temperature using a Nanoscope III SPM (Digital Instruments, Santa Barbara, CA) operated in the contact mode. For the image acquisition a standard silicon nitride probe was used with a nominal tip radius of 20–60 nm. Repeated scanning of the same polymer area showed no alteration of the surface topography due to the interaction force between the polymer and the AFM tip. The evolution of the imposed defects after heating above T_g was then recorded by AFM, following a cyclic procedure of heating the sample in an oven, quenching the sample and imaging at room temperature. Experiments were performed at 100, 105 and 110 °C.

3. Results and discussion

Fig. 1 shows the evolution of an indent upon heating above T_g, as it was recorded with AFM. Initially the indent is triangular (Fig. 1a) because a three-sided diamond pyramid tip was used for the nanoindentation. Upon heating above T_g, the indent becomes circular (Fig. 1b) and gradually it tends to result in a flat polymer surface (Fig. 1c). The corresponding cross-sections reveal that the indent 'expands' in the lateral direction with a simultaneous increase of the diameter (d) and the rim width (w). In the vertical direction both indent depth (z_A) and rim height (x) decrease with annealing time. The dynamics of the leveling process were recorded for six shallow indents induced on thick ($h = 120$ nm) and six shallow indents imposed on thin ($h = 50$ nm) films, heated at 100, 105 and 110 °C. Figs. 2 and 3 show the change of the indent depth and the radius ($R = d/2$) as a function of time. At short annealing times the indent is triangular. The calculated radii at these initial time stages correspond to the radii of the equivalent circles, which occupy area, equal to the area of the triangular projections of the indents. The data were fit with a power law equation $R \sim t^x$, with $x = 0.3$ for the thick and $x = 0.2$ for the thin films.

The leveling process decreases the mean local curvature of the system, until it becomes zero (flat polymer surface). The mean local curvature of a surface at a given point A_0, is

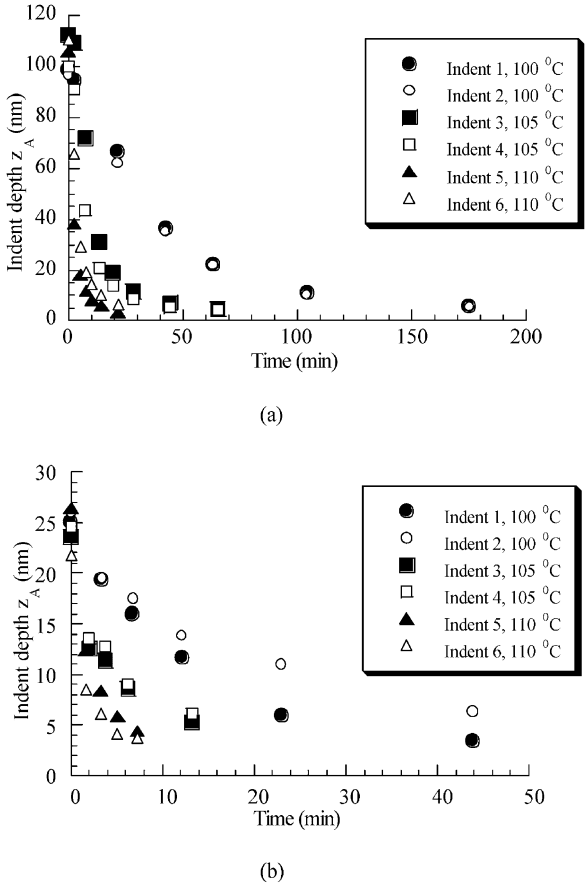

Fig. 2. Indent depth (z_A) versus time for (a) thick ($h = 120$ nm) and (b) thin ($h = 50$ nm) films. For each thickness and temperature, measurements for two indents were performed.

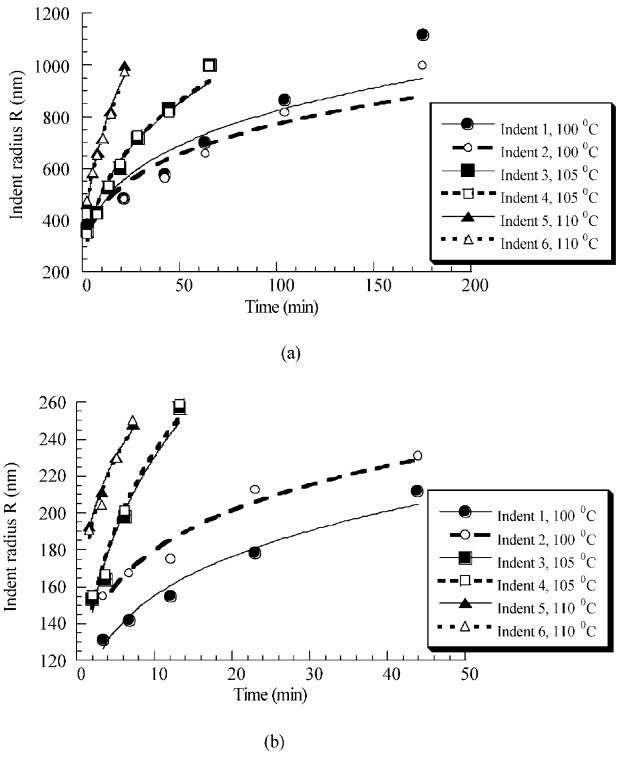

Fig. 3. Indent radius (R) for (a) thick and (b) thin films. The radius of the indent is defined at the level of the flat free polymer surface ($R = d/2$ in Fig. 1a). Data at $t = 0$ are not included. A power law fitting is shown, $R \sim t^x$ with $x = 0.3$ for (a) and $x = 0.2$ for (b). For each thickness and leveling temperature, measurements for two indents were performed.

defined as:

$$H|_{A_0} = \frac{1}{2}\left(\frac{1}{R_1}|_{A_0} + \frac{1}{R_2}|_{A_0}\right) \quad (1)$$

where R_1 is the minimal and R_2 the maximal value, of the curvature radius R, of a section normal to the surface at the point A_0. In 2D, the curvature of a curve $y = f(x)$ at a given point (x_0, y_0) is defined as:

$$\frac{1}{R}|_{(x_0,y_0)} = \frac{|f''(x_0)|}{[1 + f'(x_0)^2]^{3/2}} \quad (2)$$

Geometrically, the mean curvature of a spherical surface is constant and independent of the position. The indents that we study however have a different mean curvature at any given point. We focus on point A, which corresponds to the maximum depth of the indent (Fig. 1a) because: (i) it is the point at the indent bottom with the highest mean curvature. Therefore any effect of the curvature reduction, during the leveling process, should be more pronounced at this point and (ii) point A moves only in the perpendicular direction. During the leveling process the indents enlarge in the lateral direction and therefore all points at the free polymer surface, except point A, undergo a motion involving components in both the lateral and the vertical direction. Focusing on point A eliminates the complexities associated with the lateral motion. To find the mean curvature, we curve fit the cross-sections at the directions with minimal and maximal radii of curvature at point A with an equation $z = f(x)$. This is then used to calculate $1/R_1|_A$ and $1/R_2|_A$ from Eq. (2). The mean value H_A is calculated from Eq. (1). The complicated shape of the cross-section of an indent makes accurate curve fitting a difficult task. To simplify the problem, we focus on the bottom of the indent. That is, we curve fit only the portion $O'AO''$ (Fig. 1b) by a fourth order polynomial. We arbitrary define the bottom of the indent $O'AO''$ as the portion with a constant vertical height of 4 nm (Fig. 1b). This portion of the cross-section is adequate for our purposes, because: (i) it is a long enough portion to describe the shape of the cross-section at the vicinity of the point A and therefore a confident calculation of H_A can be performed and (ii) it can be fit by a fourth order polynomial function quite precisely and therefore the calculation of H_A using Eqs. (1) and (2) is feasible. Fig. 4 shows the decrease of the mean curvature at point A, H_A, with time, upon heating at three temperatures above T_g. Since in all cases we used the same Berkovich tip to impose the initial indents, we expect H_A at $t = 0$ (right after the nanoindentation and prior to any heating above T_g) to be constant. Indeed, the initial H_A is near $10^{-2}\,\mathrm{nm}^{-1}$ for all cases.

The indent leveling process can be interpreted in terms of a diffusion process. For isotropic materials (surface tension does not depend on the surface orientation) the classical Gibbs–Thomson equation applies [20,21]:

$$\mu = \Omega\gamma\left(\frac{1}{R_1} + \frac{1}{R_2}\right) \quad (3)$$

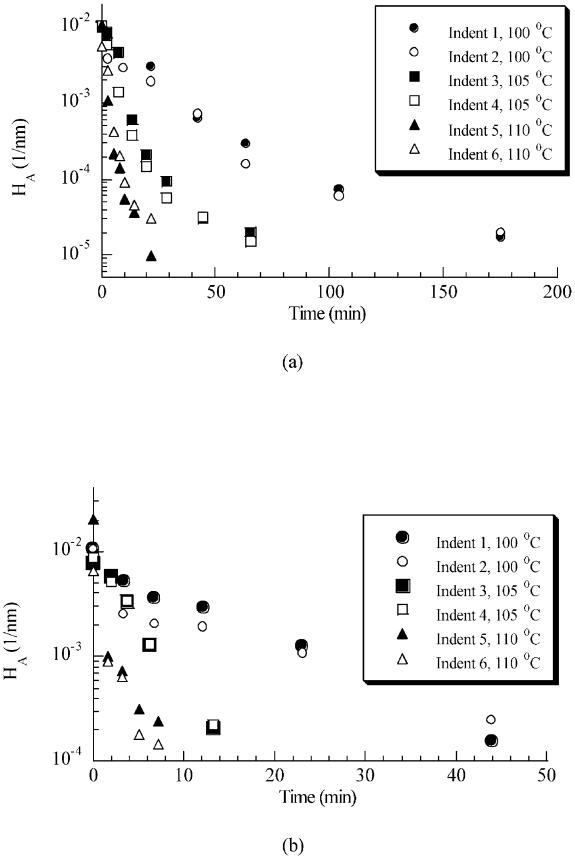

Fig. 4. Mean curvature of shallow indents at the point which corresponds to the maximum depth (point A) versus time for (a) thick and (b) thin films, in log–linear plots. At $t = 0$, H_A is near $10^{-2}\,\mathrm{nm}^{-1}$ for all cases.

where μ is the chemical potential, γ the surface tension and Ω the molecular volume. In our case, the material of interest is a polymer (PS above T_g) rather than a usual liquid. In that case, we approximate Ω by the volume occupied by a coil:

$$\Omega = \frac{4}{3}\pi R_g^3 \quad (4)$$

where R_g is the radius of gyration of the PS molecules. Eq. (3) implies that any curvature gradients are directly related to chemical potential gradients at the surface. Diffusion is driven by the need to reduce curvature. The flux of the material moving along the surface, in the x-direction, is given by the Einstein–Nernst relation as [20]:

$$J_s = \nu v = -\frac{\nu D_s}{kT}\frac{\partial \mu}{\partial x} \quad (5)$$

where v is the drift velocity, ν the surface density of the molecules participating in the diffusion, D_s the surface diffusivity and k is the Boltzmann constant. To obtain the leveling rate, as measured by the drift velocity along z (Eq. (6)) we combine Eqs. (3)–(6) to give Eq. (7):

$$v_z = \frac{dz}{dt} \quad (6)$$

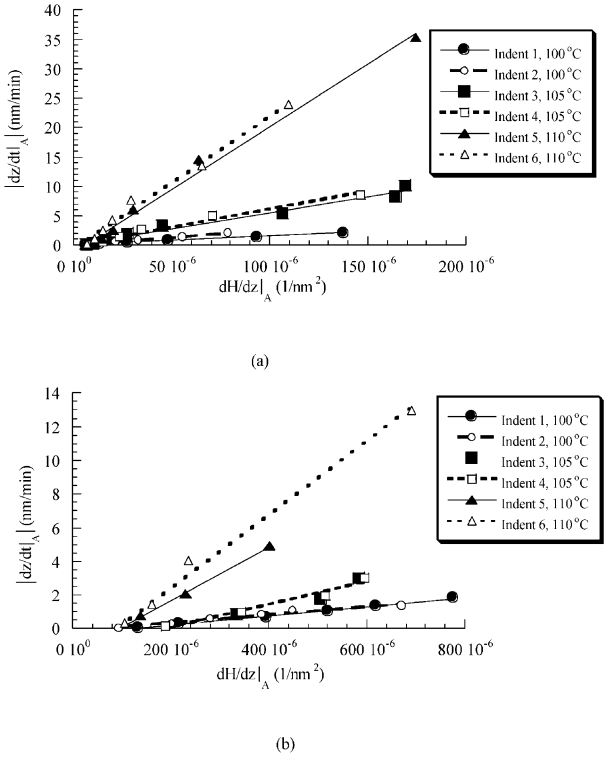

Fig. 5. Absolute value of leveling rate at point A ($|\mathrm{d}z/\mathrm{d}t|_A$) versus the mean curvature gradient in the vertical direction at point A ($\partial H/\partial z|_A$) for (a) thick and (b) thin films. Linear fits are shown.

$$\frac{\mathrm{d}z}{\mathrm{d}t} = -\frac{8\pi D_s \gamma R_g^3}{3kT}\frac{\partial H}{\partial z} \tag{7}$$

By measuring $\mathrm{d}z/\mathrm{d}t|_A$ and $\partial H/\partial z|_A$ we can calculate the diffusivity D_s. Fig. 5 shows the plots of $|\mathrm{d}z/\mathrm{d}t|_A|$ versus $\partial H/\partial z|_A$. A linear relation fits the data for each case quite well. Values for the surface tension of PS are given in Table 1 and $R_g = 3$ nm [22]. The calculated D_s values are shown in Fig. 6. For comparison, we also present the self-diffusivity of bulk PS at several temperatures, measured by Eastman and Lodge [23,24]. Eastman labeled PS molecules with a photoisomerizable dye molecule. Forced Rayleigh scattering was then used to follow the trace of the labeled molecules. The direct comparison of our data with Eastman's results required a correction in the temperature (x-axis of Fig. 6) and in the diffusion coefficient values (y-axis of Fig. 6) due to the difference in the molecular weights between our samples ($M_w = 10,900$ g/mol) and Eastman's samples ($M_w = 13,000$ g/mol). We have adjusted the difference in the glass transition temperatures by plotting in the x-axis $T–T_g$. Both samples have molecular weights lower than the chain entanglement weight. Consequently, the chains are unentangled and they follow the Rouse model ($D \sim M^{-1}$). In Fig. 6 we have adjusted the molecular weight difference in the diffusivity values by dividing the bulk diffusivity by the factor of 0.82 which is the ratio of the two molecular weights. A relatively good agreement between our results and the self-diffusivity values for bulk PS is obtained.

Table 1
Surface tension of PS (Mw = 10,900 g/mol) at several temperatures [22]

T (°C)	γ (mN/m)
100	34.3
105	34
110	33.6
120	33
130	32.3
140	31.7

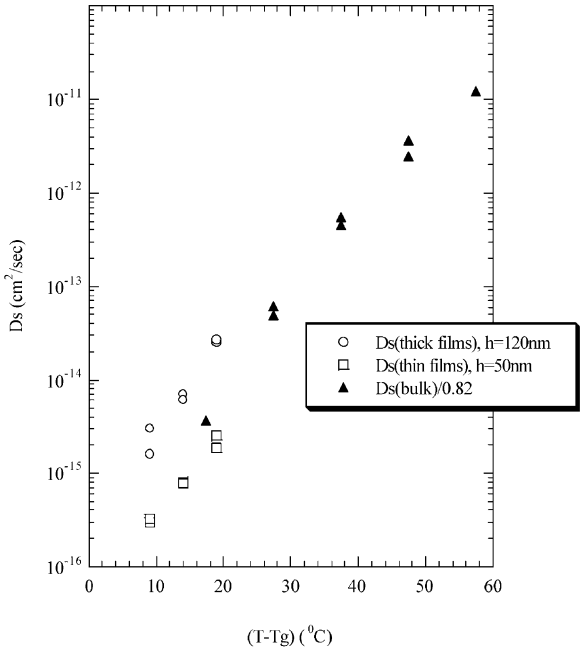

Fig. 6. D_s of PS for thick and thin films versus $T–T_g$. For comparison bulk self-diffusivity values are presented [23,24]. Bulk values have been divided by 0.82 to adjust the molecular weight difference.

Fig. 6 showed that the D_s values for the thick ($h = 120$ nm) films are higher than the corresponding values for the thin ($h = 50$ nm) films. In the following we provide two possible explanations. Except from the diffusion flux that drives the indent bottom upwards due to the curvature gradient along the vertical, z, direction, one can expect a similar flux produced by the rim relaxation. This process should increase the measured diffusivity values, depending on the size of the rim. The impact, of the flux produced by the rim relaxation, on the D_s measurements, should be higher for the 120 nm films than the thinner ones, simply because the imposed indents are deeper and consequently the rims are bigger.

Geometrical restrictions applied in the diffusion of the polymer chains due to the film thickness, may be important. The end-to-end distance (R_{EE}) of the PS was 7.5 nm, well below the film thicknesses. However in the diffusion process it is not only the film thickness which is important but also

the distance between the bottom of the indent and the substrate (distance $h - z_A$). During the leveling process, this distance ranges from 10–120 nm and 25–50 nm for the thick and thin films, respectively. Considering that the majority of the experimental measurements for the 120 nm films were performed when $h - z_A > 70\ \text{nm} = 9.3R_{EE}$, it is concluded that the effect of confining the chains motion in small volumes is more pronounced in the 50 nm films, at which $3.3R_{EE} < h - z_A < 6.7R_{EE}$. Therefore this additional obstacle in the motion of the chains should have a greater impact on the D_s values measured for the thin ($h = 50$ nm) films.

4. Conclusion

Using AFM the dynamics of the leveling process of nanoindentation induced defects on unentangled ($M\text{w} = 10,900$ g/mol) PS films was studied upon heating above T_g. The initial triangular indent evolved to circular with a simultaneous increase of its radius, R. The latter was found to scale with time, t, as $R \sim t^x$ where $x = 0.3$ for the thick ($h = 120$ nm) and $x = 0.2$ for the thin ($h = 50$ nm) films. The leveling process was described as a diffusion process, driven by the curvature gradient. The calculated diffusivity values (D_s) were found to be close to the bulk self-diffusivity values of PS. Also, thick films ($h = 120$ nm) exhibited higher D_s values than the thin ones ($h = 50$ nm). This was attributed to the rim relaxation effect and the spacing between the indent bottom and the substrate. Both effects retard the leveling process in the thin films, compared to their effect in the case of the thick films.

Acknowledgements

Support by the Center for Interfacial Engineering (CIE), a National Science Foundation Engineering Research Center is gratefully acknowledged.

References

[1] Brochard-Wyart F, Daillant J. Can J Phys 1990;68:1084–8.
[2] Redon C, Brochard-Wyart F, Rondelez F. Phys Rev Lett 1991;66:715–8.
[3] Reiter G. Phys Rev Lett 1992;68:75–8.
[4] Reiter G. Langmuir 1993;9:1344–51.
[5] Reiter G. Macromolecules 1994;27:3046–52.
[6] Redon C, Brzoska JB, Brochard-Wyart F. Macromolecules 1994;27:468–71.
[7] Sharma A, Reiter GJ. Colloid Interface Sci 1996;178:383–99.
[8] Khanna R, Sharma AJ. Colloid Interface Sci 1997;195:42–50.
[9] Stange TG, Hendrickson WA, Evans DF. Langmuir 1997;13:4459–65.
[10] Jacobs K, Mecke KR, Herminghaus S. Langmuir 1998;14:965–9.
[11] Jacobs K, Seemann R, Schatz G, Herminghaus S. Langmuir 1998;14:4961–3.
[12] Xie R, Karim A, Douglas JF, Han CC, Weiss RA. Phys Rev Lett 1998;81:1251–4.
[13] Sharma A, Khanna R. Phys Rev Lett 1998;81:3463–6.
[14] Sharma A, Khanna RJ. Chem Phys 1999;110:4929–36.
[15] Karapanagiotis I, Gerberich WW, Evans DF. Langmuir 2001;17:2375–9.
[16] Karapanagiotis I, Evans DF, Gerberich WW. Langmuir 2001;17:3266–72.
[17] Kheshgi HS. PhD Thesis. University of Minnesota, 1983.
[18] Keunings R, Bousfield DW. J Non-Newtonian Fluid Mech 1987;22:219–33.
[19] Karapanagiotis I, Evans DF, Gerberich WW. Macromolecules 2001;34:3741–7.
[20] Mullins WW. Metals Park (OH): American Society of Metals, 1963. p. 17–66.
[21] Mullins WW. J Appl Phys 1957;28:333–9.
[22] Brandrup J, Immergut EH. Polymer handbook. 3rd ed. New York: Wiley, 1989.
[23] Eastman CE, Lodge TP. Macromolecules 1994;27:5591–8.
[24] Eastman CE. PhD Thesis, University of Minnesota, 1993.